DEVELOPMENTAL DYNAMICS 232:268–281, 2005

RESEARCH ARTICLE

Control of Basement Membrane Remodeling and Epithelial Branching Morphogenesis in Embryonic Lung by Rho and Cytoskeletal Tension

Kimberly A. Moore,[1] Tom Polte,[1,2] Sui Huang,[1] Bin Shi,[1] Eben Alsberg,[1] Mary E. Sunday,[2] and Donald E. Ingber[1,2]*

Local alterations in the mechanical compliance of the basement membrane that alter the level of isometric tension in the cell have been postulated to influence tissue morphogenesis. To explore whether cell tension contributes to tissue pattern formation in vivo, we modulated cytoskeletal force generation in embryonic mouse lung (embryonic days 12–14) rudiments using inhibitors of Rho-associated kinase (ROCK), myosin light chain kinase, myosin ATPase, and microfilament integrity, or a Rho stimulator (cytotoxic necrotizing factor-1). Tension inhibition resulted in loss of normal differentials in basement membrane thickness, inhibition of new terminal bud formation, and disorganization of epithelial growth patterns as well as disruption of capillary blood vessels. In contrast, increasing cell tension through Rho activation, as confirmed by quantitation of myosin light chain phosphorylation and immunohistocytochemical analysis of actin organization, accelerated lung branching and increase capillary elongation. These data suggest that changes in cytoskeletal tension mediated by Rho signaling through ROCK may play an important role in the establishment of the spatial differentials in cell growth and extracellular matrix remodeling that drive embryonic lung development. *Developmental Dynamics 232:268–281, 2005.* © 2004 Wiley-Liss, Inc.

Key words: Rho-associated kinase; myosin light chain phosphorylation; contractility; extracellular matrix; mechanoregulation; pattern formation; angiogenesis; capillary; prestress

Received 27 May 2004; Accepted 18 August 2004

INTRODUCTION

Morphogenesis of epithelial tissues is made possible through the establishment of local differentials in cell proliferation that appear to be mediated through spatial control of extracellular matrix (ECM) turnover (Ingber and Jamieson, 1985; Huang and Ingber, 1999). Regions with the most rapid ECM turnover exhibit both basement membrane thinning and enhanced proliferation rates within adjacent epithelial cells (Bernfield et al., 1972; Mollard and Dziadek, 1998; Nogawa et al., 1998); due to coupling between new ECM synthesis and degradation, these regions expand to form new buds and lobules in developing glands. Moreover, basement membrane breakdown accompanies Mullerian duct involution (Ikawa et al., 1984), and complete dissolution of this ECM using pharmacological agents promotes regression of both growing mammary epithelium (Wicha et al., 1980) and angiogenic capillary blood vessels (Ingber et al., 1986).

Although the mechanisms that establish this crucial spatial heterogeneity of growth based on ECM remodeling in the tissue microenvironment remain poorly understood, local changes in ECM *mechanics* could con-

[1]Vascular Biology Program, Department of Surgery, Children's Hospital and Harvard Medical School, Boston, Massachusetts
[2]Department of Pathology, Children's Hospital and Harvard Medical School, Boston, Massachusetts
Grant sponsor: National Institutes of Health; Grant numbers: HL67669; HL44984.
***Correspondence to: Donald E. Ingber, M.D., Ph.D., Vascular Biology Program, Karp Family Research Laboratories, Room 11-127, Children's Hospital, 300 Longwood Avenue, Boston, MA 02115. E-mail: donald.ingber@childrens.harvard.edu**

DOI 10.1002/dvdy.20237
Published online 20 December 2004 in Wiley InterScience (www.interscience.wiley.com).

tribute to this process. Developing epithelial tissues exist in a state of isometric tension or "prestress" due to tractional forces that are generated within the cytoskeleton of their constituent cells, transmitted across transmembrane integrin receptors, and resisted by the neighboring ECM (Ash et al., 1973; Banerjee et al., 1977; Ingber and Jamieson, 1985; Ingber, 2003). Because the basement membrane is under tension, local ECM degradation will result in local basement membrane thinning and expansion of this weakened microdomain, producing a dehiscence much like a "run in a stocking." Because the ECM normally resists and balances cell tractional forces, changes in ECM mechanics will feed back to promote cell distortion or alter the level of isometric tension in the cytoskeleton (Ingber, 2003). For example, increased compliance of the ECM may result in stretching of the ECM as well as spreading of adjacent adherent cells and associated cytoskeletal reorganization. Importantly, in vitro studies have shown that cell and cytoskeletal distortion (spreading) makes epithelial and endothelial cells sensitive to mitogens and permits cell cycle progression (Huang et al., 1998; Huang and Ingber, 1999), whereas cell retraction (as occurs when basement membranes fully dissolve during tissue involution; Ingber et al., 1986) promotes differentiation or apoptosis (Ben-Ze'ev et al., 1980, 1988; Peterson et al., 1992; Singhvi et al., 1994; Li et al., 1997; Chen et al., 1997; Huang et al., 1998). Changes in ECM compliance and cell distortion also can influence cell motility (Pelham and Wang, 1997, 1999; Parker et al., 2002).

In addition, alterations in the balance of mechanical forces transmitted across transmembrane integrin receptors can influence cytoskeletal tension generation by means of activation of myosin light chain (MLC) phosphorylation (Chrzanowska-Wodnicka and Burridge, 1996; Bershadsky et al., 1996; Polte et al., 2004). The tractional forces that cells exert on the ECM also feed back to alter ECM structure by modulating expression of genes that encode ECM proteins (Chiquet et al., 1996), promoting ECM fibril assembly (Halliday and Tomasek, 1995), altering metalloproteinase activities (Brown and Hudlicka, 2003; Yamaguchi et al., 2002), and mechanically unraveling molecular domains within individual ECM proteins that modulate fibril assembly (Baneyx and Vogel, 1999).

Importantly, disruption of the cytoskeleton or interference with cytoskeletal tension generation inhibits cell cycle progression in cultured cells (Guadagno and Assoian, 1991; Assoian and Zhu, 1997; Huang et al., 1998; Welsh et al., 2001; Numaguchi et al., 2003) as well as epithelial morphogenesis in embryonic salivary gland (Ash et al., 1973). Mechanical tension generated in the cytoskeleton and exerted by cells on their adhesions in the cerebral cortex also drives gyrus formation in the developing brain (Van Essen et al., 1998). Thus, cytoskeletal tension may represent a potential control point for local modulation of cell growth and ECM remodeling during morphogenesis.

Analysis of control of cytoskeletal tension generation in contractile cells has traditionally focused on the role of intracellular calcium and myosin light chain kinase (MLCK; De Lanerolle et al., 1991; Stull et al., 1988). More recently, a new pathway has been described that involves the small GTPase Rho, which promotes MLCK phosphorylation and stimulates cytoskeletal contraction through activation of Rho-associated kinase (ROCK) and subsequent inhibition of MLC phosphatase (Amano et al., 1996; Kimura et al., 1996). Rho and ROCK mediate the effects of altering mechanical force transfer across integrins on MLC phosphorylation and focal adhesion assembly in cultured cells (Chrzanowska-Wodnicka and Burridge, 1996; Bershadsky et al., 1996; Elbaum et al., 1999; Helfman et al., 1999; Riveline et al., 2001; Tan et al., 2003). Rho has a role in early embryogenesis, as evidenced by its requirement for head formation in *Xenopus* embryos (Wunnenberg-Stapleton et al., 1999). Active Rho also appears to be required for normal development during early stages of chick and mouse embryonic morphogenesis (Wei et al., 2001).

Given the important role of cytoskeletal tension in cell growth control and ECM remodeling within cultured cells and its role in early development, we reasoned that Rho-dependent tension generation also might be important for branching tissue morphogenesis in the developing lung during later stages of embryogenesis. Preliminary studies demonstrated that cytotoxic necrotizing factor-1 (CNF-1), a general Rho activator, accelerated epithelial branch formation in cultured embryonic lung rudiments (Moore et al., 2002). Here, we address the question of whether modulating cytoskeletal tension generation by means of Rho or other pathways impacts cell proliferation, ECM structure, and pattern formation within the growing epithelium, endothelium, and mesenchyme of the developing mouse lung. The results reveal that Rho-dependent cytoskeletal tension generation is critical for the establishment of local differentials of cell growth and basement membrane thickness as well as normal tissue pattern formation during lung morphogenesis.

RESULTS

Control of Lung Branching Morphogenesis

Mouse lung buds were dissected and placed in culture at embryonic day (E) 12 when the trachea, primary bronchi, and five lobes had formed; at this point, >90% of the buds had 9–13 peripheral branch points (Fig. 1A). The branching pattern of the primary bronchial buds was monopodial, whereas the secondary bronchi underwent dichotomous branching. Analysis of serial light microscopic images revealed that each bud enlarged and formed clefts resulting in two or three smaller buds within 48 hr (Fig. 1A,B). Over this time course, there was greater than a threefold (217 ± 25%) increase in the number of peripheral branches relative to time 0 (Fig. 2).

To explore whether Rho-mediated control of cytoskeletal contractility plays a role in tissue morphogenesis, lung buds were cultured in the presence of increasing doses of the ROCK inhibitor Y27632, which inhibits MLC phosphorylation and tension generation (Somlyo et al., 2000). Lung bud formation was reduced by more than half in lungs treated with Y27632, and the effect was dose-dependent (Fig. 2).

In contrast to controls that increased their terminal bud count by more than 200% at 48 hr, lungs treated with 10 μM, 20 μM, and 40 μM Y27632 increased only by 117 ± 24%, 92 ± 23%, and 69 ± 17%, respectively ($P < 0.01$). Microscopic analysis of lungs treated with the highest dose (40 μM) of Y27632 revealed the presence of slightly enlarged epithelial buds that failed to form clefts when compared with controls (Fig. 3). This effect also appeared to be specific (i.e., not due to generalized toxicity) as these effects on tissue morphology were reversible when Y27632 was washed out after 18 hr, and lungs were examined at 48 hr (Fig. 4A). There was a dramatic change after the wash out of the drug that was marked by the reformation of clefts and smaller lung buds that appeared similar to untreated controls in terms of number and size of buds (Fig. 4A,B).

Importantly, three other modulators of cytoskeletal tension generation that act by distinct mechanisms all inhibited branching morphogenesis by 24 hr. When growing lungs were treated with cytochalasin D (100 ng/ml), a drug that disrupts actin microfilament integrity, almost complete inhibition of morphogenesis was observed (Fig. 3). Similar inhibition of epithelial development was observed in lungs treated with 20 mM 2,3-butanedione 2-monoxime (BDM), which interferes with cytoskeletal tension generation by inhibiting myosin ATPase (Riccio et al., 1999), or with 20 μM ML-9, which inhibits MLCK (Saitoh et al., 1987; Fig. 3). Again, these effects were found to be dose-dependent (not shown), and the inhibitory effects of all compounds were either partially or completely reversed when drugs were washed out after 18 hr ($P < 0.01$; Fig. 4B). However, the loss of the appearance of a distinct epithelium at 48 hr suggests that these less-specific inhibitors may have produced significant toxicity at this later time.

The inhibition of epithelial branching by blocking the Rho effector ROCK with Y27632 is consistent with our previous demonstration that increasing cell tension by treatment with CNF-1, a bacterial toxin that activates Rho family GTPases, accelerates embryonic lung branching morphogenesis (Moore et al., 2002). Here, we analyzed this process in greater detail and found that treated lungs exhibited a dose-dependent, biphasic response: low doses (2 and 20 ng/ml) CNF-1 produced a significant ($P < 0.05$) 2.4-fold increase in terminal bud number, whereas an extremely high dose (200 ng/ml) inhibited this process relative to untreated controls ($P < 0.001$)(Fig. 5A,B). Moreover, at the highest dose of CNF-1, the whole lung explant physically contracted (Fig. 5B), apparently as a result of excessive tension generation throughout the entire gland.

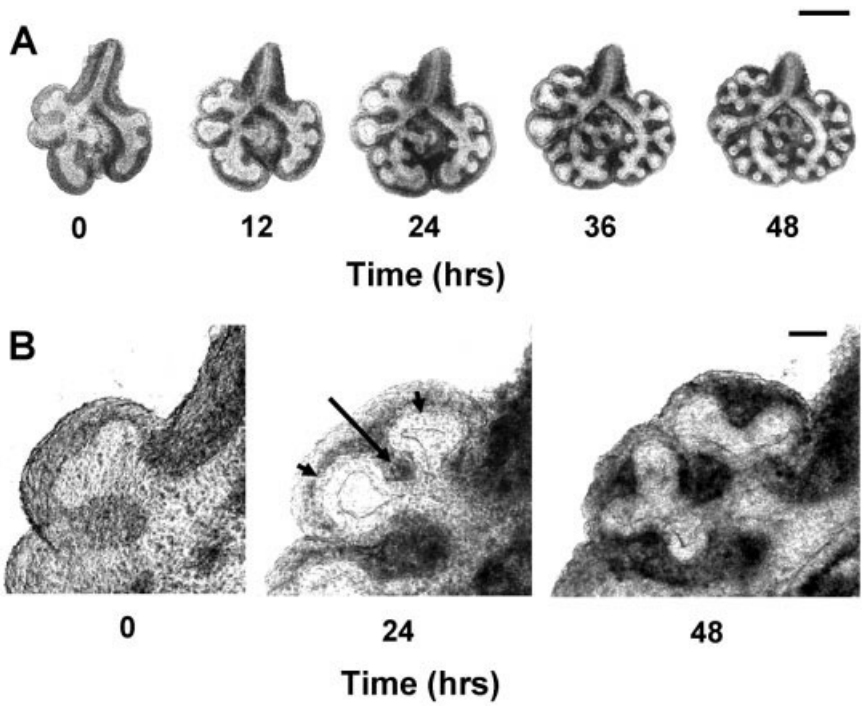

Fig. 1. Normal lung morphogenesis over 48 hr as monitored by serial light microscopy. **A:** Photographs recorded every 12 hr reveal that normal branching morphogenesis results from bud enlargement and expansion, followed by cleft formation at each bud's tip which produces two or three smaller buds. **B:** Higher magnification views of individual buds from glands shown in A. The long arrow indicates the cleft between two adjacent buds (short arrows) in the growing epithelium after 24 hr of culture. Scale bars = 500 μm in A, 50 μm in B.

Correlation Between Morphogenetic Effects and Changes in MLC Phosphorylation

To confirm that the observed effects on morphogenesis were mediated by changes in cytoskeletal tension, as opposed to other Rho activities, we directly measured MLC phosphorylation in these developing glands. Lungs treated with CNF-1 for 48 hr exhibited a dose-dependent increase in

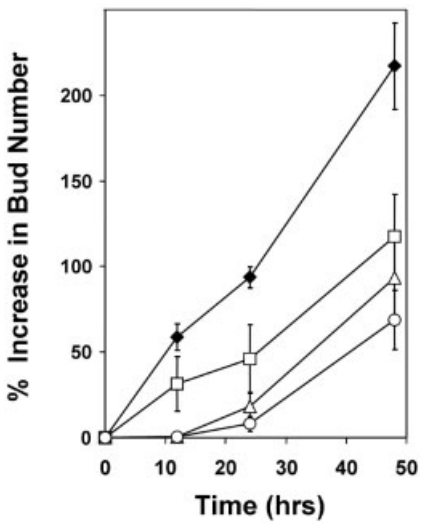

Fig. 2. Treatment of lung explants with the Rho-associated kinase inhibitor Y27632 inhibits epithelial branching morphogenesis. Compared with untreated controls (diamonds), lung buds treated with Y27632 (10 μM, squares; 20 μM, triangles; 40 μM, circles) exhibited a significant dose-dependent reduction in the relative increase in number of terminal lung buds at all time points ($P < 0.01$). Results are expressed as the mean percentage increase in number of terminal lung buds formed at each branch point relative to Time 0 baseline controls (error bars indicate SEM).

MLC phosphorylation relative to untreated controls as the dose was raised from 2 to 200 ng/ml (Fig. 6). Quantification of signal intensity of both the mono-phosphorylated and di-phosphorylated isoforms of MLC also revealed a small (less that twofold) but statistically significant ($P < 0.05$) increase in the number of moles of PO_4 per mole of MLC in lungs treated with 2 and 20 ng/ml CNF-1 compared with control lungs. In contrast, treatment of lungs with 40 μM Y27632 completely abolished MLC phosphorylation ($P < 0.01$; Fig. 6).

These effects on MLC phosphorylation at the level of the whole gland also correlated with local changes in cytoskeletal organization measured with anti-actin antibodies at the cellular level. These histocytochemical studies revealed cortical actin staining in all control cells, with the greatest intensity of linear staining appearing within the mesenchymal cells that underline the expanding regions at the tip of the growing epithelium (Fig. 7). This level of actin staining was greatly enhanced in cells treated with CNF-1, again particularly within the cells of the subepithelium, whereas all actin staining was no longer detectable after Y27632-treatment (Fig. 7). Thus, regional variations in cytoskeletal organization appear to exist in normal growing lung epithelium, and both CNF-1 and Y27632 can influence these structural gradients.

To determine whether the effects on lung development we observed scaled with Rho activation, we measured Rho activity in lung lysates using the Rhotekin-binding assay (Ren et al., 1999). As expected, increasing doses of CNF-1 significantly elevated Rho activity in a dose-dependent manner (Fig. 8). However, quantification of these data revealed that Rho activity levels saturated at the intermediate dose of 20 ng/ml, even though the lowest dose of CNF-1 produced the greatest effects on epithelial budding (Fig. 5). Low dose CNF-1 (2 ng/ml) increased Rho activity by 2.25-fold relative to controls ($P < 0.05$), whereas a higher dose (20 ng/ml) increased Rho activity by 3.76-fold ($P < 0.007$), and an even higher dose of CNF-1 (200 ng/ml) did not produce any additional Rho activation. Although Rho activity was optimal at the highest dose of CNF-1, the level of cytoskeletal contractility (as measured by MLC activity) appeared to dominate, causing inhibition of growth and gross contraction of the gland (Moore et al., 2002). Thus, budding morphogenesis appeared to be promoted by low levels of Rho activation that produced moderate increases in MLC phosphorylation (tension generation) sufficient to increase isometric tension within the cells of growing gland but not great enough to drive global tissue contraction.

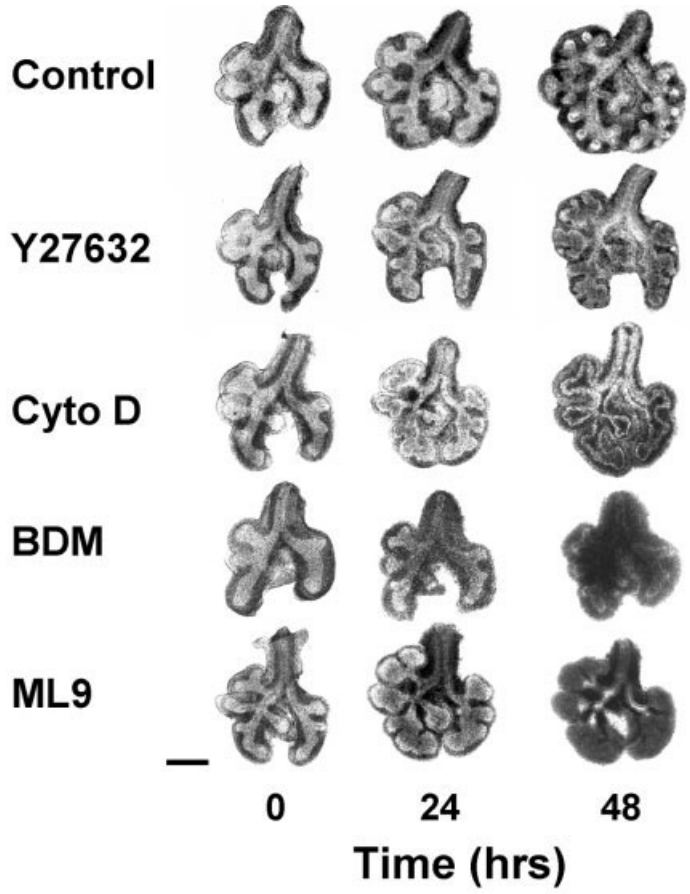

Fig. 3. Treatment with agents that disrupt or suppress cytoskeletal tension generation by various mechanisms inhibit lung morphogenesis. Lungs treated with Y27632 (40 μM) for 24 hr or more exhibited enlarged bud ends and failed to form normal clefts and tight, symmetric outpouchings as seen in control lungs. Treatment with cytochalasin D (100 ng/ml; Cyto D), 2,3-butanedione 2-monoxime (BDM, 20 mM), or ML9 (20 μM) completely prevented increases in epithelial bud number and size over a similar time course. Scale bar = 500 μm.

Tension-Dependent Control of ECM Structure and Cell Growth Patterns

To compare the effects of Rho activation and ROCK inhibition on epithelial and mesenchymal cell growth, 5-bromo-2′-deoxyuridine (BrdU) incorporation was analyzed within histological sections that were also stained with antibodies to laminin to delineate the epithelial basement membrane boundary. Immunohistochemical studies confirmed that the epithelium of the normal lung grew as a folded, hollow tube that exhibited enhanced cell proliferation rates within localized regions along their periphery, as indicated by BrdU staining (Fig. 9A,F). BrdU incorporation also was observed within the mesenchymal tissue, although no discrete spatial patterns could be detected. Importantly, the peripheral regions of the epithelium that contained the most rapidly growing cells corresponded to areas of the epithelium that were underlined by thinner regions of the basement membrane (Fig. 9A,F); this finding was even more

clear when sections were stained only for laminin (Fig. 10A,E).

CNF-1–treated lungs that exhibited enhanced budding maintained normal spatial differentials of cell growth and basement membrane structure. In lungs treated with CNF-1 at both 2 ng/ml (Fig. 9B,G) and 20 ng/ml (Fig. 9F,H), normal spatial differentials of epithelial cell proliferation were maintained as growing cells remained concentrated within the expanding tips of the growing epithelial buds located at the periphery of the lung rudiment. Moreover, the spatial correlation between regions of highest cell proliferation and greatest basement membrane thinning at the gland periphery also was maintained (Fig. 9C,H).

Most importantly, quantitation of BrdU labeling revealed that CNF-1 did not produce its accelerating effects on budding morphogenesis by producing a generalized increase in cell proliferation. The lowest dose of CNF-1 (2 ng/ml) that stimulated the greatest increase in epithelial budding (Fig. 5) did not alter the total rate of cell proliferation (Fig. 9K). There was a significant increase in the epithelial BrdU labeling index in lungs treated with CNF-1 at 20 ng/ml (18.5 ± 3% vs. 8.1 ± 3% in controls; $P < 0.001$; Fig. 9K); however, this dose produced a much smaller increase in epithelial budding than the lowest CNF-1 dose (Fig. 5). Mesenchymal cell growth was not altered under any condition (Fig. 9K).

In contrast, treatment of growing lungs with the ROCK inhibitor Y27632 (40 μM) resulted in loss of these normal local differentials in cell growth, piling up of both BrDU-labeled and nonlabeled epithelial cells within the lumen and, hence, abnormal epithelial patterning (Fig. 9D,I). Inhibition of tension generation also resulted in loss of the normal spatial differentials in ECM remodeling, such that basement membrane thickness appeared relatively constant along the entire epithelium (Fig. 10B,F). Moreover, ROCK inhibition produced these effects on epithelial development without producing a statistically significant change in epithelial proliferation (Fig. 9K). Mesenchymal cell growth also remained nearly constant in untreated and Y27632-treated lungs (Fig. 9K). Thus, the disturbed morphogenesis caused by inhibition of ROCK and cytoskeletal tension generation did not appear to be due to global inhibition of cell proliferation, whereas it correlated directly with loss of normal spatial differentials of both cell growth (BrdU incorporation) and ECM remodeling. Finally, although Y27632 treatment inhibited basement membrane thinning, disrupted normal growth differentials, and inhibited budding morphogenesis (Figs. 9D,I, 10B,F), this effect reversed upon drug wash out (Fig. 9E,J). Localized basement membrane thinning was restored in the tips of growing buds at the periphery of the gland, resulting in normal branching morphogenesis (Fig. 10C,G).

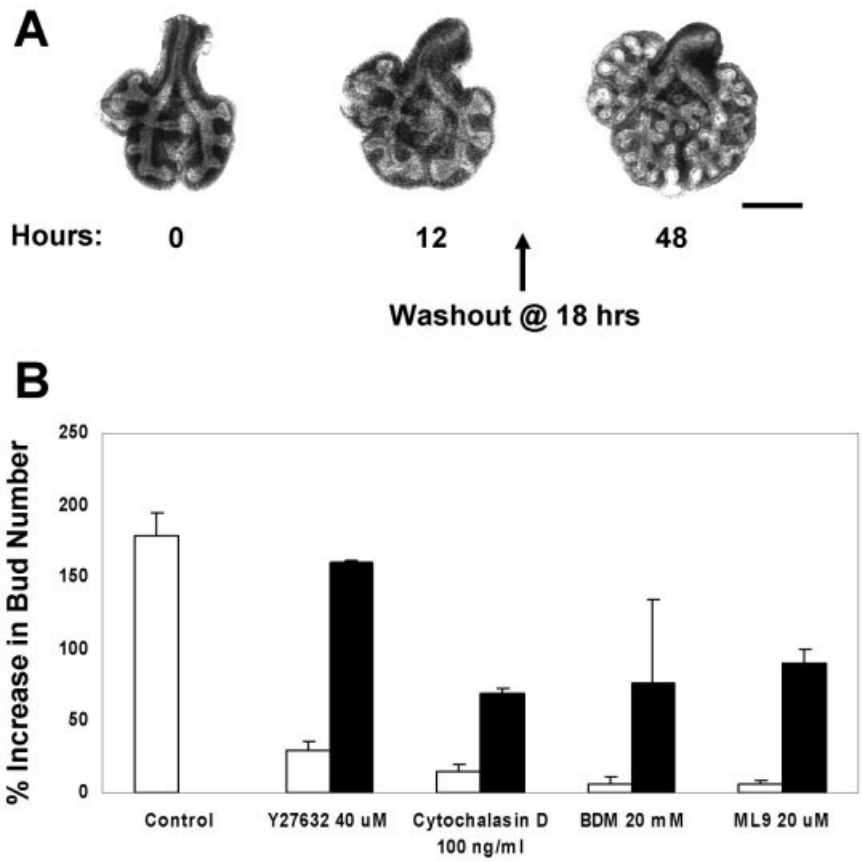

Fig. 4. The effects of the different tension inhibitors and cytoskeletal disruptors on lung branching are reversible. **A:** Serial light microscopic photographs show that the suppression of epithelial branching produced by Y27632 (40 μM) was almost completely reversed when the drug was washed out after 18 hr and replaced with normal culture medium. **B:** Morphometric quantitation of results of reversibility studies demonstrate that the inhibitory effects of Y27632 (40 μM), cytochalasin D (100 ng/ml), 2,3-butanedione 2-monoxime (BDM, 20 mM), or ML9 (20 μM) were all partially or completely reversible at 48 hr after each of the pharmacological agents was washed out at 18 hr ($P < 0.01$). Results are expressed as the mean percentage increase in number of terminal lung buds formed at each branch point relative to Time 0 baseline controls (white bars, continuous exposure to agents or control conditions for 48 hr; black bars, 18 hr exposure to agent, followed by 30 hr in control conditions; error bars indicate SEM). Scale bar = 500 μm in A.

The laminin staining also revealed the existence of branching capillary networks in regions between neighboring epithelial buds in normal cultured glands (Fig. 9), and this was confirmed by CD31 staining (not shown). In control lungs, endothelial cells within the mesenchyme aligned circumferentially in an orderly manner within capillary networks that surrounded the outer surface of each epithelial bud (Fig. 9A,F). CNF-1 treatment appeared to promote further extension and elongation of these networks to match extension of the epithelium (Fig. 9B,C,G,H). Conversely, ROCK inhibition resulted in disorganization of vascular architecture and disruption of the capillary network formation (Fig. 9D,I). In

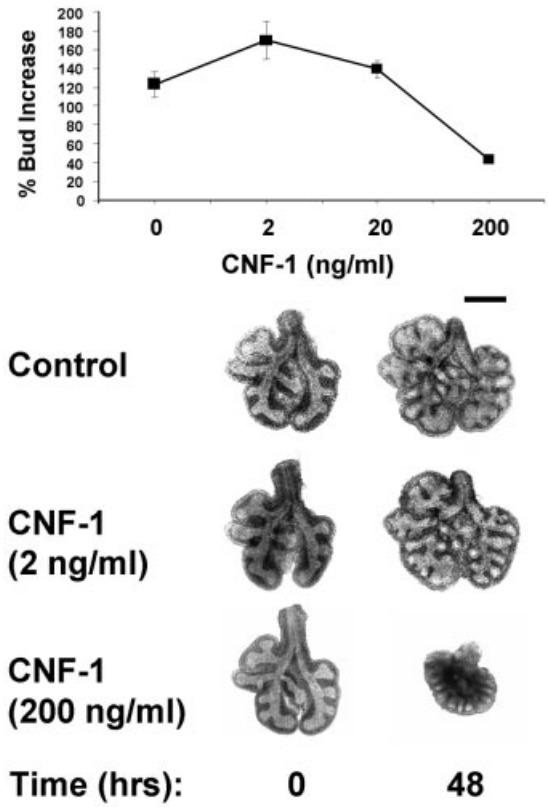

Fig. 5. Effects of activating Rho using cytotoxic necrotizing factor-1 (CNF-1) on lung development. Top: CNF-1–treated lungs exhibited a dose-dependent, biphasic response in that low doses (2 and 20 ng/ml) produced a significant increase in terminal bud number ($P < 0.05$), whereas an extremely high dose (200 ng/ml) inhibited this process relative to untreated controls ($P < 0.001$). Results are expressed as the mean percentage increase in number of terminal lung buds formed at each branch point relative to Time 0 baseline controls. Bottom: Photomicrographs of lung rudiments cultured for 48 hr in the presence or absence of 2 or 200 ng/ml CNF-1. Note the increase in distal lung buds at the low dose, and the large-scale contraction of the entire gland at the highest dose after 48 hr of drug exposure. Scale bar = 500 μm.

Y27632-treated lungs, endothelial cells appeared as isolated cells that appeared to be bunched together (Fig. 9D,I), and this effect was reversible when the drug was washed out (Fig. 9E,J).

DISCUSSION

The results of this study suggest that cytoskeletal tension controlled by the Rho-ROCK pathway is a critical developmental regulator during branching morphogenesis in embryonic mouse lung. Lung development was inhibited in organ culture when intracellular tension was dissipated by treatment of cells with various pharmacological inhibitors of actomyosin-based tension generation, and when the actin cytoskeleton was chemically disrupted. The demonstration that a variety of agents which act on different molecular targets in the contractility pathway, including MLC kinase, myosin ATPase, and ROCK, all produced similar effects suggest that the modulation of cell tension is the central mechanism of action of these drugs. This finding was supported by the demonstration that effects on lung growth and expansion correlated more closely with MLC phosphorylation (i.e., through both inhibition and stimulation of cytoskeletal contractility) and with local changes in actin staining, than with the level of Rho activation.

Spatial differentials in cell proliferation and basement membrane turnover are normally observed in the periphery of growing epithelium, causing these areas to expand more rapidly than surrounding portions of the epithelium and ultimately to form new buds in many embryonic glands (Bernfield et al., 1984). Treatment of growing lung epithelium with the ROCK inhibitor Y27632 resulted in a significant and reversible decrease in the number of terminal lung buds and in marked morphological alterations: the buds were enlarged and failed to form clefts. Histological analysis revealed loss of all cortical (linear) actin staining and total disorganization of epithelial morphology with piling up of cells within the lumen as well as inhibition of angiogenesis, as indicated by disruption of the vascular architecture of the lung bud. This finding was accompanied by loss of spatial differentials in both cell growth and basement membrane remodeling. Specifically, treatment with Y-27632 resulted in the appearance of a basement membrane of abnormally constant thickness throughout the gland, along with the presence of proliferating (BrdU-incorporating) cells throughout the tissue parenchyma rather than only at the expanding edge. The endothelial cells that normally align within continuous branching capillary networks along the periphery of the epithelium in untreated lungs also appeared disorganized and lacked their normal branching patterns in these lungs.

Importantly, cell proliferation rates were not significantly altered when ROCK was inhibited, even though normal pattern formation was prevented. This finding is consistent with the finding that blocking ROCK with Y27632 does not significantly inhibit cell proliferation in vitro (Somlyo et al., 2000). That Y27632 eliminated all measurable levels of MLC phosphorylation and cortical actin staining, combined with the finding that multiple different inhibitors of tension generation produced similar effects, strongly suggest that ROCK inhibition altered lung development by interfering with cytoskeletal force generation. In other words, ROCK inhibition specifically suppressed the force that is responsible for establishment of the spatial differentials in basement membrane structure and cell growth that drive bud formation.

The mechanism by which cell tension can influence the establishment of cell growth patterns remains unclear. However, a theoretical micromechanical control mechanism has

been proposed that could explain this response (Fig. 11; Ingber and Jamieson, 1985; Huang and Ingber, 1999; Alsberg et al., 2004). This hypothesis is based on the past observation that basement membrane thinning in regions of most rapid tissue expansion results from enhanced local ECM turnover (Bernfield et al., 1972, 1984; Ash et al., 1973; Banerjee et al., 1977). The regions of the basement membrane that experience increased degradation and lose structural materials should exhibit increased mechanical compliance or distensibility (Ingber and Jamieson, 1985; Huang and Ingber, 1999). Importantly, the basement membrane is normally tensionally prestressed (exists in a state of isometric tension), because the neighboring epithelial and mesenchymal cells exert tractional forces on their ECM adhesions (Huang and Ingber, 1999; Moore et al., 2002). Thus, because of the action of tractional forces exerted by the neighboring adherent cells, structurally compromised regions of the basement membrane where turnover is greatest should spread out and thin more than neighboring regions, much like a "run" in a woman's stocking (Fig. 11). This change, in turn, would alter isometric tension in the cytoskeleton or promote local distortion of neighboring adherent cells, making these cells preferentially susceptible to growth stimuli (Ingber and Jamieson, 1985; Chen et al., 1997; Huang et al., 1998). In this manner, cell tension would contribute directly to the establishment of the spatial growth differentials that drive tissue branching and that were lost when tension generation was inhibited in the present study.

Our finding that inhibition of cell tractional forces with Y27632 both inhibited the enhanced linear actin staining normally exhibited by mesenchymal cells underlining the tip of growing buds and prevented local basement membrane thinning in these regions is consistent with this micromechanical control hypothesis (i.e., without tension, the stocking would not "run" even if structural materials are removed locally). The existence of local *mechanical* differentials along the basement membrane during tissue morphogenesis is also supported by the past finding that tenascin-C, which increases its expression levels in response to mechanical tension in vitro (Chiquet-Ehrismann et al., 1994), is normally expressed at high levels at the tips of growing epithelial buds where laminin levels are lowest during an earlier stage of embryonic lung development (Koch et al., 1991). On the other hand, the changes in basement membrane thinning we observed in Y27632-treated glands could equally be explained by tension-dependent inhibition of ECM turnover, either alone or in combination with decreased traction of the basement membrane. This explanation is possible because past studies have shown that changes in mechanical forces can influence many steps in ECM production and remodeling (Halliday and Tomasek, 1995; Chiquet et al., 1996; Baneyx and Vogel, 1999; Yamaguchi et al., 2002; Brown and Hudlicka, 2003).

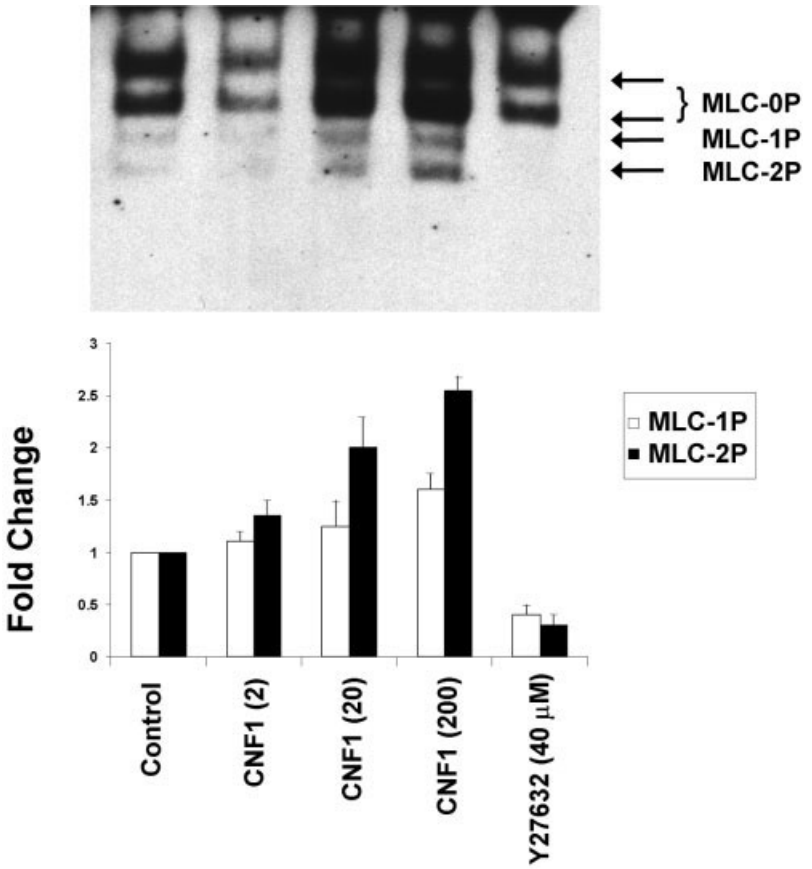

Fig. 6. Effects of cytotoxic necrotizing factor-1 (CNF-1) and Y27632 on myosin light chain (MLC) phosphorylation in developing lung. A representative Western blot (top) and densitometric analysis of data from multiple experiments (bottom) show that lungs treated with CNF-1 for 48 hr exhibited a significant dose-dependent increase in MLC phosphorylation of both the single (MLC-1P) and double (MLC-2P) phosphorylated isoforms (arrows) relative to the unphosphorylated form (MLC-0P) at all doses used compared with untreated controls ($P < 0.05$). In contrast, treatment of lungs with Y27632 (40 μM) fully inhibited phosphorylation of both the mono- and di-phosphorylated isoforms of MLC ($P < 0.01$). Results are represented as fold-change of number of moles PO_4 per mole of MLC compared with untreated controls.

We have shown previously that activation of Rho with low doses (2 to 20 ng/ml) of CNF-1 results in acceleration of epithelial bud formation in E12–E14 embryonic lung, whereas a higher dose induces compaction of the entire organ and suppresses morphogenesis (Moore et al., 2002). In this study, we extended this work by first confirming that CNF-1 does in fact activate Rho in these lung rudiments using a direct Rhotekin-based Rho activity assay. Interestingly, although development of the epithelium was significantly accelerated, the basement membrane in the distal portions of the CNF-1–treated lung buds continued to exhibit pronounced thinning

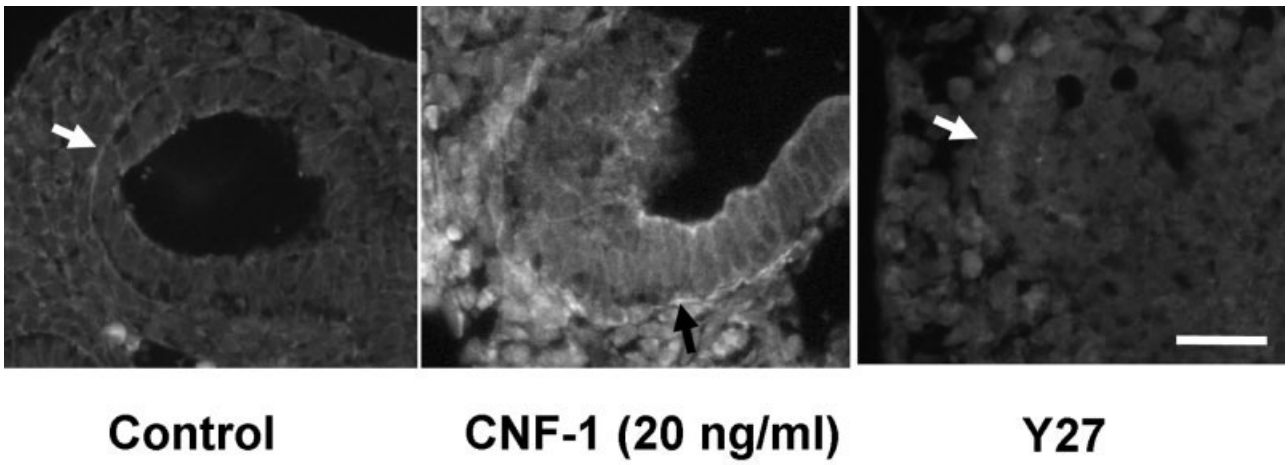

Fig. 7. Effect of cytoskeletal tension modulators on cytoskeletal organization. Immunofluorescence photomicrographs of histological sections of lungs treated for 48 hr without (control) or with cytotoxic necrotizing factor-1 (CNF-1, 20 ng/ml) or Y27632 (40 μM) and stained for cytoskeletal actin. Note that cortical actin staining was detectable in all control cells, with a relative enhancement of staining intensity within mesenchymal cells directly beneath the basement membrane at the tip of the growing gland. This subepithelial staining was further enhanced with CNF-1 treatment, whereas all detectable linear actin staining was lost after addition of Y27632 (tips of arrows abut on basement membrane). Scale bar = 50 μm.

as seen in the controls. The organization of the microvasculature also appeared more advanced in terms of the degree of extension and elongation of the capillary network. This latter result is consistent with the finding that capillary sprout formation can be stimulated by application of tensional forces (Yamaguchi et al., 2002; Brown and Hudlicka, 2003). These results on capillary development in this three-dimensional organ culture system also confirm the findings of various in vitro studies, which suggest that cell spreading and changes in cytoskeletal tension can influence capillary endothelial cell proliferation (Ingber et al., 1986; Ingber, 1990; Chen et al., 1997; Huang et al., 1998; Numaguchi et al., 2003). Finally, it is important to note that the bimodal effects of CNF-1 on morphogenesis and organ size correlated more closely with its effects on MLC phosphorylation than on Rho activity or the total rate of cell proliferation. Specifically, the maximal stimulation of morphogenesis produced by low CNF-1 dose (2 ng/ml) was associated with a suboptimal effect on Rho, and no detectable effect on cell growth. Furthermore, increasing the dose of CNF-1 from 20 to 200 ng/ml had no additive effect on Rho activation, whereas it both enhanced MLC phosphorylation and induced contraction of the entire gland. These data lend additional support to the micromechanical control model in which cell-generated contractile forces play a central role in the establishment of the local growth differentials that drive tissue development.

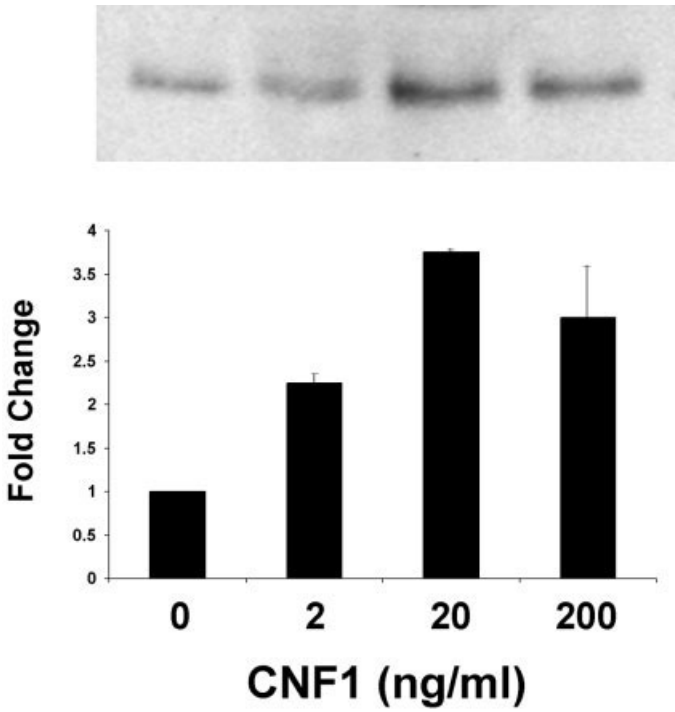

Fig. 8. Activation of Rho activity in lung rudiments by cytotoxic necrotizing factor-1 (CNF-1). A representative Western blot (top) and densitometric analysis of data from multiple experiments confirm that CNF-1 increases Rho activity significantly in a dose-dependent manner, saturating at doses of 20 ng/ml and greater ($P < 0.007$), as detected by using the Rhotekin-binding assay.

Rho A has been linked previously to the maintenance of epithelial morphology and polarity by taking part in the epithelial-mesenchymal interactions that control morphogenesis in developing kidney (Bianchi et al., 2003) and salivary gland (Menko et al., 2001). Rho signaling is also thought to be involved in the development of the phenotype of mice containing a targeted mutation in the α3β1 integrin gene (Menko et al.,

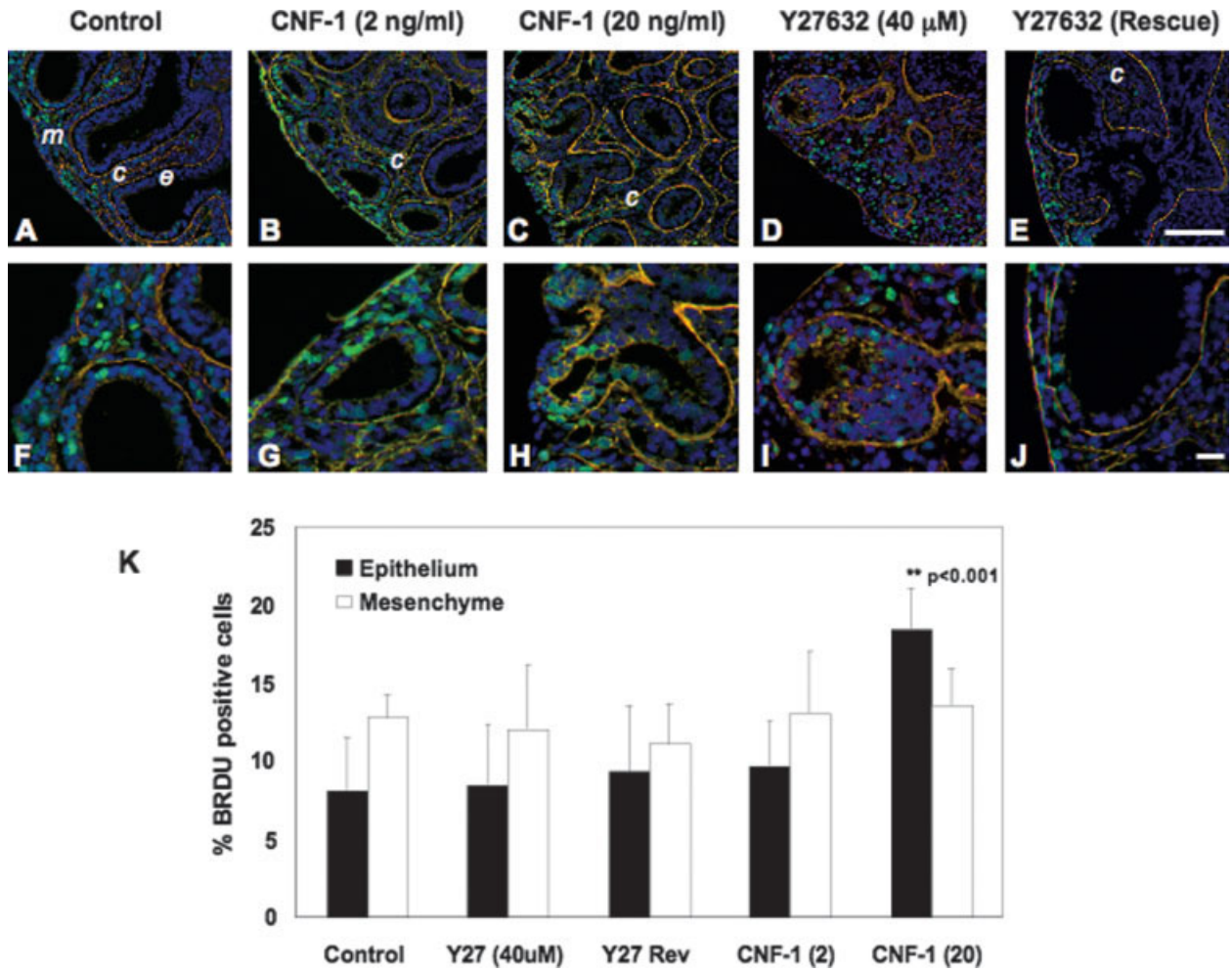
Control
CNF-1 (2 ng/ml)
CNF-1 (20 ng/ml)
Y27632 (40 μM)
Y27632 (Rescue)
m
c
e
A
B
C
D
E
F
G
H
I
J
K
Epithelium
Mesenchyme
** p<0.001
% BRDU positive cells
25
20
15
10
5
0
Control
Y27 (40uM)
Y27 Rev
CNF-1 (2)
CNF-1 (20)

Fig. 9.

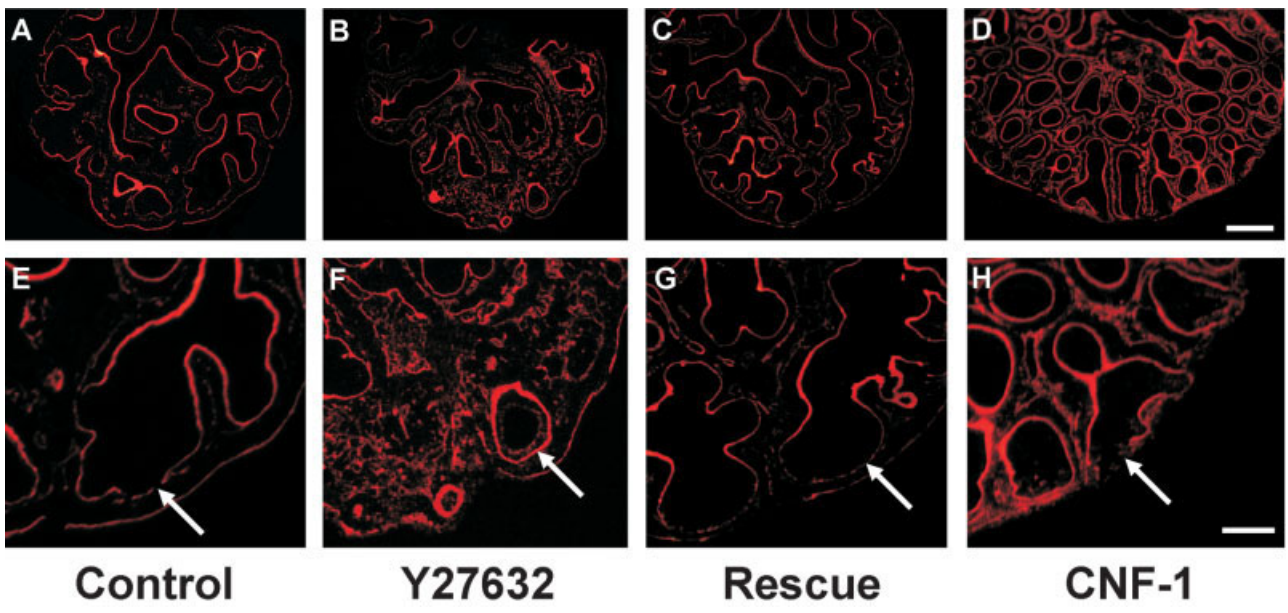
A
B
C
D
E
F
G
H
Control
Y27632
Rescue
CNF-1

Fig. 10.

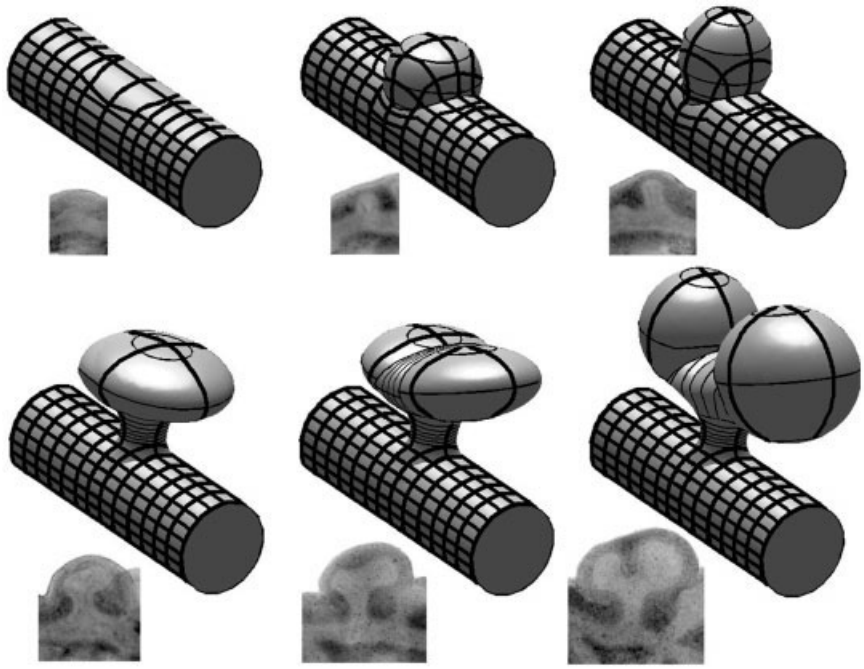

Fig. 11. Mechanical contributions to epithelial tissue morphogenesis. Top: Theoretical mechanical strain distributions within the basement membrane of the developing lung epithelium at different times during branching morphogenesis. Bottom: Photomicrographs of individual buds show the sequential structural alterations that exhibit similar morphogenetic changes during mouse lung development. An increased spacing between the strain field lines indicates regions where the basement membrane loses it mechanical stiffness, thins, and experiences increased mechanical strain (distortion). Note that regions of increased strain correlate precisely with regions of epithelial expansion and new bud formation. Increased basement deposition results in decreased strain in the proximal stalks of newly formed buds and in the intervening clefts. Changes in basement membrane strain may alter cell growth through associated stress-dependent changes in the cytoskeleton and cell distortion (see Ingber and Jamieson, 1985; Huang and Ingber, 1999; and Alsberg et al., 2004, for more details).

2001). This mutation leads to abnormal disruptions in the basement membrane, disorganization of acini within the mesenchyme, and perinatal death (Kreidberg et al., 1996; DiPersio et al., 1997; Menko et al., 2001). We found that epithelial and endothelial organization are both lost in Y27632-treated lungs; coordinated disruption of epithelium and developing vascular networks has been similarly observed in past studies on fetal lung morphogenesis (Schwarz et al., 2003). These findings provide further support for Rho as an integral player in the control of epithelial–stromal interactions during tissue development and specifically suggest that the ROCK effector pathway responsible for control of cytoskeletal contractility is critical for this control.

Although it is important to note that CNF-1 activates other small GTPases (e.g., Rac and Cdc42) in addition to Rho (Doye et al., 2002), our work with Y27632 clearly demonstrates that the Rho–ROCK–MLC pathway is required for normal epithelial and endothelial morphogenesis in the embryonic lung. At least six substrates of ROCK may play a role in actin cytoskeletal reorganization and contractility associated with lung morphogenesis: MLC kinase (Amano et al., 1996), MLC phosphatase (Kimura et al., 1996), LIM-kinase

Fig. 9. Effects of cytotoxic necrotizing factor-1 (CNF-1) and Y27632 on cell growth in developing lung rudiments. Top: Histochemical analysis of growth and basement membrane remodeling, as detected by immunofluorescence staining for 5-bromo-2′-deoxyuridine (BrdU) incorporation (green) and laminin (red) at low (A–E) and high magnification (F–J). DAPI (4′,6-diamidine-2-phenylidole-dihydrochloride) staining was used for nuclear identification (blue). **A,F:** Control lung contained the greatest number of growing cells along the periphery of the growing epithelium in regions in which basement membrane thinning was observed. Well-developed capillaries (*c*) surrounded by their own basement membrane can been seen within the mesenchyme (*m*) between adjacent epithelial buds (*e*). **B,C,G,H:** Treatment with CNF-1 at 2 ng/ml (B,G) and 20 ng/ml (C,H) resulted in increased numbers of epithelial buds; however, only the higher dose exhibited greater numbers of proliferating cells. At both doses, the proliferating cells remained localized to the periphery of the gland near regions of basement membrane thinning. CNF-1 treatment appeared to promote further extension and elongation of these capillary networks (*c*) in parallel with extension of the epithelium. **D,I:** Treatment with Y27632 inhibited basement membrane thinning and resulted in piled up clusters of disorganized cells that filled much of the epithelial lumen. Proliferative cells were still detected; however, their normal spatial localization to the periphery was lost. Rho-associated kinase inhibition also resulted in disorganization of vascular architecture and disruption of the capillary network formation; endothelial cells appeared to be bunched together within isolated clusters of cells. **E,J:** When glands were washed free of Y27632 after 18 hr of exposure, and cultured for 30 additional hr, local differentials in both basement membrane thickness and cell proliferation were restored; this restoration was accompanied by reinitiation of branching morphogenesis and reappearance of well-formed capillary networks (*c*). **K:** Morphometric quantitation of these results revealed that none of the drug treatments produced a significant change in the total level of BrdU incorporation within either epithelial or mesenchymal cells, except for the 20 ng/ml CNF-1 dose, which increased epithelial cell proliferation without changing mesenchymal growth ($P < 0.001$). Scale bars = 50 μm in E (applies to A–E), 10 μm in J (applies to F–J).

Fig. 10. A–F: Effects of Y27632 and cytotoxic necrotizing factor-1 (CNF-1) on basement membrane structure as detected by immunofluorescence staining for laminin, viewed at low (A–D) and high (E–H) magnification. Arrow indicates a region of the basement membrane at the periphery of one bud within each gland in E–H. **A,E:** The thinnest regions of the basement membrane typically underlie the peripheral regions of the epithelium (arrow) where the most rapid epithelial growth rates were observed as shown in Figure 1. **B,F:** Inhibition of cytoskeletal tension generation by treatment with Y27632 resulted in loss of the normal differentials in basement membrane structure, such that a thick continuous linear pattern of laminin staining was observed surrounding all epithelium. **C,G:** The normal thinning of the basement membrane at the periphery of the gland was restored after glands were washed free of Y27632, and morphogenesis was reinitiated. **D,H:** Basement membrane thinning also was maintained at the periphery of growing epithelium in lungs treated with CNF-1 (20 ng/ml). Scale bars = 250 μm in D (applies to A–D), 100 μm in H (applies to E–H).

(Maekawa et al., 1999), adducin (Kimura et al., 1998), the ERM (ezrin/radixin/moesin) family of proteins (Matsui et al., 1998), and a Na+/H+ exchanger (Tominaga et al., 1998). Based on the finding that other modulators of the contractility pathway also inhibited lung budding, we believe that MLC kinase and phosphatase are likely to be critical mediators of these effects; however, other targets could also be involved. In any case, our results clearly demonstrate that Rho and its downstream target ROCK are essential for normal tissue development in the embryonic mouse lung.

One interesting finding in this study is that inhibition of Rho by treatment with Y27632 feeds back to inhibit local basement membrane thinning. This thinning inhibition could be due to either increased synthesis or decreased degradation of the basement membrane or to inhibition of cell traction forces as described above. Local ECM remodeling is mediated by local changes in ECM degrading enzymes, such as matrix metalloproteinases (MMPs; Lee et al., 2001), which have been implicated in tissue morphogenesis in a variety of organs. One hypothesis, then, is that basement membrane thinning results from tension-dependent increases in MMP activity. However, tension from integrin binding and cell spreading actually results in decreased levels of MMP-2 activity through decreased expression of MT1-MMP mRNA in endothelial cells (Yan et al., 2000). Moreover, mechanical tension seems to prevent degradation of matrix by MMP activity in other cell types (Von den Hoff, 2003). Thus, inhibition of localized basement membrane thinning after tension inhibition would suggest that these two morphogenetic events are coupled. As seen in this study, this could indicate that cells need to pull on the basement membrane in the presence of ongoing degradation to produce dehiscence of the basement membrane and the subsequent "run in the stocking" phenomenon. On the other hand, cyclic strain up-regulates the expression of MT1-MMP in microvascular endothelial cells during angiogenesis (Yamaguchi et al., 2002). MMP expression is also up-regulated during involution, which is made possible through increased ECM degradation and remodeling (Talhouk et al., 1991; Lund et al., 1996). Therefore, this mechanism will require future study.

Organogenesis in the embryo involves the precise temporal and spatial coordination of cell growth to create functional tissue architecture (Huang and Ingber, 1999). To generate structures that exhibit localized bending, budding, or branching, one cell or a small group of cells must divide to expand tissue mass, while its immediate neighbors must remain quiescent. This coordination requires that each cell correctly interpret multiple mechanical and chemical cues from its microenvironment. Past work has focused on regional production of growth factors as directional guides for branching in the developing lung (Metzger and Krasnow, 1999). However, sharp growth differentials responsible for tissue patterning exist only micrometers apart, thereby requiring physical signals in the microenvironment to provide a mechanism for local control. The results of the present study suggest that mechanical interactions between cells and the ECM in the tissue microenvironment may contribute significantly to this response. In fact, it is well documented that mechanical variables, including lung volume, fetal breathing movements, the size of the intrathoracic space, and amniotic fluid volume, regulate normal fetal lung growth and development (Nobuhara and Wilson, 1996). Moreover, increasing mechanical distension by tracheal occlusion or continuous intrapulmonary perfluorocarbon accelerates lung growth and differentiation in animal models (Sakakura et al., 1976; Cai et al., 1998; Nogawa et al., 1998; Sanchez-Esteban et al., 1998) and in human infants (Bullard et al., 1997; Wirtz and Dobbs, 2000). Conversely, pathological conditions that compromise the normal balance of forces within embryonic lungs may interfere with this process, inhibit normal tissue development, and result in pulmonary hypoplasia, a major cause of death in the neonate with congenital diaphragmatic hernia (Liggins, 1994). Thus, this micromechanical mechanism may have important implications for disease as well as development.

In summary, we have demonstrated that Rho regulates epithelial morphogenesis and angiogenesis in the developing lung through its ability to modulate ROCK and MLC phosphorylation, and thereby control cytoskeletal tension generation. This requires a fine balance, however. Although inhibition of tension generation prevents both localized basement membrane thinning and branching morphogenesis, very high levels of contractility results in complete retraction of the whole gland, cell rounding, and cessation of organ development. Thus, pathological conditions that compromise or alter the normal balance of forces within developing organs, either through alterations of cell tension or ECM structure, may interfere with this process and prevent normal tissue development. The recent finding that mechanical distortion of *Drosophila* embryos can alter expression of developmentally relevant genes (Farge, 2003) supports this micromechanical control hypothesis. The discovery that Rho-mediated tension regulates lung morphogenesis also may facilitate development of new approaches to prevent, minimize, or correct congenital lung anomalies, as well as pulmonary diseases in the newborn.

EXPERIMENTAL PROCEDURES

Murine Lung Bud Cultures

Embryos from day 12 (E12) timed-pregnant Swiss Webster mice (Taconic Farms, MA) were removed aseptically and placed into bacteriological dishes containing Waymouth's MB medium (Gibco/BRL). Lung rudiments were microdissected en bloc (with all lobes still attached to the trachea), washed in serum-free medium, and transferred to a semipermeable membrane (Falcon cell inserts, 0.4-μm pore size) that was placed over 2.5 ml of serum-free BGJb medium (Fitton-Jackson modification; Gibco/BRL) supplemented with penicillin, streptomycin, and ascorbic acid (0.2 mg/ml) in a six-well plate. Three lungs were placed in each well and subjected to the same dose of pharmacological agent, which was added to individual wells at 0 hr and again at 24 hr with fresh BGJb medium. The

agents included cytochalasin D (100 ng/ml; Sigma), an actin cytoskeletal disruptor; BDM (20 mM; Sigma), a myosin ATPase inhibitor known to inhibit cytoskeletal tension generation; ML9 (20 μM; Sigma), an MLCK inhibitor; Y27632 (10, 20, or 40 μM; Yoshitomi Pharmaceuticals), a highly selective ROCK inhibitor; or CNF-1 (2, 20, or 200 ng/ml; gift from Dr. K. Aktories), a Rho activator. These agents were washed out at 18 hr in some studies to check for reversibility of effects. This was repeated in three separate experiments; thus, the results presented were from a total of nine whole lungs per condition.

In vitro development was monitored within whole organs by morphological observations and serial measurements of branch points (number of buds) at 12-hr intervals from 0 to 48 hr using light microscopy; the observer was blinded to the treatment protocol. Results were expressed as percentage increase in number of terminal lung buds formed at each branch point relative to Time 0 baseline controls (n = 9 lungs/condition) ±SEM. Data were analyzed using an analysis of variance (ANOVA) single factor test and the two sample independent *t*-test. In parallel studies, lungs were fixed in 4% paraformaldehyde, paraffin-embedded, sectioned (3 μm), and stained with hematoxylin and eosin for light microscopic analysis.

Immunohistochemistry

Cellular proliferation was measured by quantifying the percentage of cells that exhibited nuclear incorporation of BrdU in control and drug-treated lungs that were pulsed with BrdU (10 μM, Amersham, Arlington Heights, IL) from hours 42–48 in culture. Lungs were fixed in 4% paraformaldehyde for 1 hr at room temperature, dehydrated, and paraffin-embedded. Three micrometer-thick sections were cut, deparaffinized, rehydrated, treated with proteinase K (10 μg/ml; Sigma) for 20 min at room temperature, blocked in TNB buffer (NEL-700A, NEN Life Sciences Products, Boston, MA), probed with a monoclonal mouse antibody against BrdU (RPN-202, Amersham) for 90 min at room temperature, detected using a biotinylated goat anti-mouse IgG antibody (BA-9200, Vector) and Texas Red–avidin (A2006, Vector), and counterstained with Hoescht (1:1,000). BrdU-positive fluorescent cells were visualized and scored using a Nikon Diaphot microscope with ×25 and ×63 objectives and the IPLab image acquisition and processing computer program (Vaytek). At least five random fields were counted per sample. Results are presented as percentage of cells incorporating BrdU ± SEM. Data were analyzed by using an ANOVA single-factor test and the two-sample independent *t*-test. Similar results were also obtained by analyzing expression of proliferating cell nuclear antigen (not shown).

To visualize laminin in basement membrane, paraffin sections were treated with proteinase K (10 μg/ml) for 20 min at room temperature, blocked in TNB buffer, probed with a rabbit polyclonal anti-laminin antibody (L9393, Sigma; 1:100), detected by using a biotinylated goat anti-rabbit antibody (BA-1000, Vector; 1:400) and Texas Red–avidin (A2006, Vector; 1:250), counterstained with Hoechst (1:1,000), and visualized by using immunofluorescence microscopy. Actin was visualized in the cytoskeleton of cells with a fluorescein isothiocyanate–conjugated monoclonal anti-actin antibody (F3046, Sigma, 1:50) in parallel sections.

Rho Activation Assay

Lungs were placed in microcentrifuge tubes and immediately crushed with a pestle for 1 min in 500 μl of lysis buffer (Rho Activation Assay Kit, Upstate Biotechnology, Lake Placid, NY) on ice, and centrifuged at 13,000 rpm for 5 min at 4°C. The supernatant was transferred to a microfuge tube, snap frozen in liquid nitrogen and stored at −80°C. When ready for analysis, 50 μl of Rhotekin RBD-agarose slurry were added and incubated for 45 min at 4°C. The beads were pelleted by centrifugation (10 sec, 14,000 rpm, 4°C), washed in lysis buffer three times, resuspended in 40 μl of Laemmli buffer, and boiled for 5 min. For Western blot analysis, protein lysates were subjected to sodium dodecyl sulfate-polyacrylamide gel electrophoresis, transferred to a TransBlot (Bio-Rad, Hercules, CA) nitrocellulose membrane, immunoblotted with an anti-Rho antibody (#06-770, Upstate Biotechnology), diluted 3 μg/ml in blocking buffer, and detected by using a horseradish peroxidase–conjugated secondary antibody (Vector) and SuperSignal Ultra (Pierce, Rockford, IL) as a chemiluminescence substrate. Signal intensity was normalized and analyzed by using NIH Image.

MLC Phosphorylation Assay

Lungs were fixed in ice-cold 10% TCA supplemented with 150 mM dithiothreitol (DTT; Sigma), immediately crushed with a pestle for 1 min, centrifuged at 13,000 rpm for 15 min at 4°C, and washed with ice cold ddH_2O, followed by two washes of acetone. The pellets were dried and stored at −20°C. Samples were then placed in sample buffer (10 M urea [#161-0730, Bio-Rad], 1× Tris-glycine running buffer, 150 mM DTT, 0.01% bromophenol blue), sonicated, loaded onto and run on electrophoretic gels at 6 mA, transferred to nitrocellulose in 1× Tris/glycine buffer with 20% methanol, blocked in 3% bovine serum albumin/Tris buffered saline, probed with an antibody to detect phosphorylated isoforms of MLC (MY-21, Sigma; 1:200) for 2 hr at room temperature, detected by using a horseradish peroxidase–conjugated secondary antibody (NA-131, Amersham; 1:4,000) and Renaissance Enhanced Luminol Reagent (NEN Life Sciences Products) as a chemiluminescent substrate. Signal intensity was normalized and analyzed by using NIH Image. Results are represented as fold-change of number of moles PO_4 per mole of MLC compared with untreated controls.

ACKNOWLEDGMENTS

We thank J. Nisbet for her assistance compiling this manuscript for publication. M.E.S. and D.E.I. were funded by grants from NIH, and K.A.M. received a Howard Hughes Medical Institute Postdoctoral Fellowship for Physicians.

REFERENCES

Alsberg E, Moore K, Huang S, Polte T, Ingber DE. 2004. The mechanical and cytoskeletal basis of lung morphogenesis. In: Massaro DJ, Massaro GD, Cham-

bon P, editors. Lung development and regeneration. New York: Marcel Dekker. p 247–274.

Amano M, Ito M, Kimura K, Fukata Y, Chihara K, Nakano T, Matsuura Y, Kaibuchi K. 1996. Phosphorylation and activation of myosin by Rho-associated kinase (Rho kinase). J Biol Chem 271: 20246–20249.

Ash JF, Spooner BS, Wessels NK. 1973. Effects of papaverine and calcium-free medium on salivary gland morphogenesis. Dev Biol 33:463–469.

Assoian RK, Zhu X. 1997. Cell anchorage and the cytoskeleton as partners in growth factor dependent cell cycle progression. Curr Opin Cell Biol 9:93–98.

Banerjee SD, Cohn RH, Bernfield MR. 1977. Basal lamina of embryonic salivary epithelia. Production by the epithelium and role in maintaining lobular morphology. J Cell Biol 73:445–463.

Baneyx G, Vogel V. 1999. Self-assembly of fibronectin into fibrillar networks underneath dipalmitoyl phosphatidylcholine monolayers: role of lipid matrix and tensile forces. Proc Natl Acad Sci U S A 96:12518–12523.

Ben-Ze'ev A, Farmer SR, Penman S. 1980. Protein synthesis requires cell-surface contact while nuclear events respond to cell shape in anchorage-dependent fibroblasts. Cell 21:365–372.

Ben-Ze'ev A, Robinson GS, Bucher NL, Farmer SR. 1988. Cell–cell and cell–matrix interactions differentially regulate the expression of hepatic and cytoskeletal genes in primary cultures of rate hepatocytes. Proc Natl Acad Sci U S A 85:2161–2165.

Bernfield MR, Banerjee SD, Cohn RH. 1972. Dependence of salivary epithelial morphology and branching morphogenesis upon acid mucopolysaccharide-protein proteoglycan at the epithelial surface. J Cell Biol 52:674–689.

Bernfield MR, Banerjee SD, Koda JE, Rapraeger AC. 1984. Remodeling of the basement membrane: morphogenesis maturation. Ciba Found Symp 108:179–196.

Bershadsky A, Chausovsky A, Becker E, Lyubimova A, Geiger B. 1996. Involvement of microtubules in the control of adhesion-dependent signal transduction. Curr Biol 6:1279–1289.

Bianchi F, Mattii L, D'Alessandro D, Moscato S, Segnani C, Dolfi A, Bernardini N. 2003. Cellular and subcellular localization of the small G protein RhoA in the human and rat embryonic and adult kidney. Acta Histochem 105:89–97.

Brown MD, Hudlicka O. 2003. Modulation of physiological angiogenesis in skeletal muscle by mechanical forces: involvement of VEGF and metalloproteinases. Angiogenesis 6:1–14.

Bullard KM, Sonne J, Hawgood S, Harrison MR, Adzick NS. 1997. Tracheal ligation increases cell proliferation but decreases surfactant protein in fetal murine lungs. J Pediatr Surg 32:207–211.

Cai S, Pestic-Dragovich L, O'Donnell ME, Wang N, Ingber D, Elson E, De Lanerolle P. 1998. Regulation of cytoskeletal mechanics and cell growth by myosin light chain phosphorylation. Am J Physiol 275: C1349–C1356.

Chen CS, Mrksich M, Huang S, Whitesides GM, Ingber DE. 1997. Geometric control of cell life and death. Science 276:1425–1428.

Chiquet-Ehrismann R, Tannheimer M, Koch M, Brunner A, Spring J, Martin D, Baumgartner S, Chiquet M. 1994. Tenascin-C expression by fibroblasts is elevated in stressed collagen gels. J Cell Biol 127:2093–2101.

Chiquet M, Matthisson M, Koch M, Tannheimer M, Chiquet-Ehrismann R. 1996. Regulation of extracellular matrix synthesis by mechanical stress. Biochem Cell Biol 74:737–744.

Chrzanowska-Wodnicka M, Burridge K. 1996. Rho-stimulated contractility drives the formation of stress fibers and focal adhesions. J Cell Biol 133:1403–1415.

De Lanerolle P, Strauss JD, Felsen R, Doerman GE, Paul RJ. 1991. Effects of antibodies to myosin light chain kinase on contractility and myosin phosphorylation in chemically permeabilized smooth muscle. Circ Res 68:457–465.

DiPersio CM, Hodivala-Dilke KM, Jaenisch R, Kreidberg JA, Hynes RO. 1997. Alpha3beta1 integrin is required for normal development of the epidermal basement membrane. J Cell Biol 137:729–742.

Doye A, Mettouchi A, Bossis G, Clement R, Buisson-Touati C, Flatau G, Gagnoux L, Piechaczyk M, Bouquet P, Lemichez E. 2002. CNF1 exploits the ubiquitin-proteasome machinery to restrict Rho GTPase activation for bacterial host cell invasion. Cell 111:553–564.

Elbaum M, Chausovsky A, Levy ET, Shtutman M, Bershadsky AD. 1999. Microtubule involvement in regulating cell contractility and adhesion-dependent signalling: a possible mechanism for polarization of cell motility. Biochem Soc Symp 65:147–172.

Farge E. 2003. Mechanical induction of Twist in the Drosophila foregut/stomodeal primordium. Curr Biol 13:1365–1377.

Guadagno TM, Assoian RK. 1991. G1/S control of anchorage-independent growth in the fibroblast cell cycle. J Cell Biol 115: 1419–1425.

Halliday NL, Tomasek JJ. 1995. Mechanical properties of the extracellular matrix influence fibronectin fibril assembly in vitro. Exp Cell Res 217:109–117.

Helfman DM, Levy ET, Berthier C, Shtutman M, Riveline D, Grosheva I, Lachish-Zalait A, Elbaum M, Bershadsky AD. 1999. Caldesmon inhibits nonmuscle cell contractility and interferes with the formation of focal adhesions. Mol Biol Cell 10:3097–3112.

Huang S, Ingber DE. 1999. The structural and mechanical complexity of cell-growth control. Nat Cell Biol 1:E131–E138.

Huang S, Chen CS, Ingber DE. 1998. Control of cyclin D1, p27kip1, and cell cycle progression in human capillary endothelial cells by cell shape and cytoskeletal tension. Mol Biol Cell 9:3179–3193.

Ikawa H, Trelstad RL, Hutson JM, Manganaro TF, Donahoe PK. 1984. Changing patterns of fibronectin, laminin, type IV collagen, and a basement membrane proteoglycan during rat Mullerian duct regression. Dev Biol 102:260–263.

Ingber DE. 1990. Fibronectin controls capillary endothelial cell growth by modulating cell shape. Proc Natl Acad Sci U S A 8:3579–3583.

Ingber DE. 2003. Mechanosensation through integrins: cells act locally but think globally. Proc Natl Acad Sci U S A 100:1472–1474.

Ingber DE, Jamieson JD. 1985. Cells as tensegrity structures: architectural regulation of histodifferentiation by physical forces transduced over basement membrane. In: Anderson LC, Gahmberg CG, Ekblom P, editors. Gene expression during normal and malignant differentiation. Orlando: Academic Press. p 13–32.

Ingber DE, Madri JA, Folkman J. 1986. A possible mechanism for inhibition of angiogenesis by angiostatic steroids; induction of capillary basement membrane dissolution. Endocrinology 119:1768–1775.

Kimura K, Ito M, Amano M, Chihara K, Fukata Y, Nakafuku M, Yamamori B, Feng J, Nakano T, Okawa K, Iwamatsu A, Kaibuchi K. 1996. Regulation of myosin phosphatase by Rho and Rho associated kinase (Rho kinase). Science 273: 245–248.

Kimura K, Fukata Y, Matsuoka Y, Bennett V, Matsuura Y, Okawa K, Iwamatsu A, Kaibuchi K. 1998. Regulation of the association of adducin with actin filaments by Rho-associated kinase (Rho-kinase) and myosin phosphatase. J Biol Chem 273:5542–5548.

Koch M, Wehrle-Haller B, Baumgartner S, Spring J, Brubacher D, Chiquet M. 1991. Epithelial synthesis of tenascin at tips of growing bronchi and graded accumulation in basement membrane and mesenchyme. Exp Cell Res 194:297–300.

Kreidberg JA, Donovan MJ, Goldstein SL, Rennke H, Shepherd K, Jones RC, Jaenisch R. 1996. Alpha 3 beta 1 integrin has a crucial role in kidney and lung organogenesis. Development 122:3537–3547.

Lee PP, Hwang JJ, Mead L, Ip MM. 2001. Functional role of matrix metalloproteinases (MMPs) in mammary epithelial cell development. J Cell Physiol 188:75–88.

Li ML, Aggeler J, Farson DA, Hatier C, Hassell J, Bissell MJ. 1987. Influence of a reconstituted basement membrane and its components on casein gene expression and secretion in mouse mammary epithelial cells. Proc Natl Acad Sci U S A 84:136–140.

Liggins GC. 1994. Growth of the fetal lung. J Dev Physiol 6:237–248.

Lund LR, Romer J, Thomasset N, Solberg H, Pyke C, Bissell MJ, Dano K, Werb Z.

1996. Two distinct phases of apoptosis in mammary gland involution: proteinase-independent and -dependent pathways. Development 122:181–193.

Maekawa M, Ishizaki T, Boku S, Watanabe N, Fujita A, Iwamatsu A, Obinata T, Ohashi K, Mizuno K, Narumiya S. 1999. Signaling from Rho to the actin cytoskeleton through protein kinases ROCK and LIM-kinase. Science 285:895–898.

Matsui T, Maeda M, Doi Y, Yonemura S, Amano M, Kaibuchi K, Tsukita S, Tsukita S. 1998. Rho-kinase phosphorylates COOH-terminal threonines of ezrin/radixin/moesin (ERM) proteins and regulates their head-to-tail association. J Cell Biol 140:647–657.

Menko AS, Kreidberg JA, Ryan TT, Van Bockstaele E, Kukuruzinska MA. 2001. Loss of alpha3beta1 integrin function results in an altered differentiation program in the mouse submandibular gland. Dev Dyn 220:337–349.

Metzger RJ, Krasnow MA. 1999. Genetic control of branching morphogenesis. Science 284:1635–1639.

Mollard R, Dziadek M. 1998. A correlation between epithelial proliferation rates, basement membrane component localization patterns, and morphogenetic potential in the embryonic mouse lung. Am J Respir Cell Mol Biol 19:71–82.

Moore KA, Huang S, Kong YP, Sunday ME, Ingber DE. 2002. Control of embryonic lung branching morphogenesis by the Rho activator, cytotoxic necrotizing factor 1. J Surg Res 194:95–100.

Nobuhara KK, Wilson JM. 1996. The effect of mechanical forces on in utero lung growth in congenital diaphragmatic hernia. Clin Perinatol 23:741–752.

Nogawa H, Morita K, Cardoso WV. 1998. Bud formation precedes the appearance of differential cell proliferation during branching morphogenesis of mouse lung epithelium in vitro. Dev Dyn 13:228–235.

Numaguchi Y, Huang S, Polte TR, Eichler GS, Wang N, Ingber DE. 2003. Caldesmon- dependent switching between capillary endothelial cell growth and apoptosis through modulation of cell shape and contractility. Angiogenesis 6:55–64.

Parker KK, Brock AL, Brangwynne C, Mannix RJ, Wang N, Ostuni E, Geisse NA, Adams JC, Whitesides GM, Ingber DE. 2002. Directional control of lamellipodia extension by constraining cell shape and orienting cell tractional forces. FASEB J 16:1195–1204.

Pelham RJ Jr, Wang Y. 1997. Cell locomotion and focal adhesions are regulated by substrate flexibility. Proc Natl Acad Sci U S A 94:13661–13665.

Pelham RJ Jr, Wang Y. 1999. High resolution detection of mechanical forces exerted by locomoting fibroblasts on the substrate. Mol Biol Cell 10:935–945.

Petersen O, Ronnov-Jessen L, Howlett AR, Bissell MJ. 1992. Interaction with basement membrane serves to rapidly distinguish growth and differentiation pattern of normal and malignant human breast epithelial cells. Proc Natl Acad Sci U S A 89:9064–9068.

Polte TR, Eichler GS, Wang N, Ingber DE. 2004. Extracellular matrix controls myosin light chain phosphorylation and cell contractility through modulation of cell shape and cytoskeletal prestress. Am J Physiol Cell Physiol 286:C518–C528.

Ren XD, Kiosses WB, Schwartz MA. 1999. Regulation of the small GTP-binding protein Rho by cell adhesion and the cytoskeleton. EMBO J 18:578–585.

Riccio ML, Koller ML, Gilmour RF Jr. 1999. Electrical restitution and spatiotemporal organization during ventricular fibrillation. Circ Res 84:955–963.

Riveline D, Zamir E, Balaban NQ, Schwarz US, Ishizaki T, Narumiya S, Kam Z, Geiger B, Bershadsky AD. 2001. Focal contacts as mechanosensors: externally applied local mechanical force induces growth of focal contacts by an mDia1-dependent and ROCK-independent mechanism. J Cell Biol 153:1175–1186.

Saitoh M, Ishikawa T, Matsushima S, Naka M, Hidaka H. 1987. Selective inhibition of catalytic activity of smooth muscle myosin light chain kinase. J Biol Chem 262:7796–7801.

Sakakura T, Nishizura Y, Dawe C. 1976. Mesenchyme-dependent morphogenesis and epithelium-specific cytodifferentiation in mouse mammary gland. Science 194:1439–1441.

Sanchez-Esteban J, Tsai SW, Sang J, Qin J, Torday JS, Rubin LP. 1998. Effects of mechanical forces on lung-specific gene expression. Am J Med Sci 316:200–204.

Schwarz MA, Wan Z, Liu J, Lee MK. 2003. Epithelial-mesenchymal interactions are linked to neovascularization. Am J Respir Cell Mol Biol [Epub].

Singhvi R, Kumar A, Lopez G, Stephanopoulos GN, Wang N, Whitesides GM, Ingber DE. 1994. Engineering cell shape and function. Science 264:696–698.

Somlyo AV, Bradshaw D, Ramos S, Murphy C, Myers CE, Somlyo AP. 2000. Rho-kinase inhibitor retards migration and in vivo dissemination of human prostate cancer cells. Biochem Biophys Res Commun 269:652–659.

Stull JT, Kamm KE, Taylor DA. 1988. Calcium control of smooth muscle contractility. Am J Med Sci 296:241–245.

Talhouk RS, Chin JR, Unemori EN, Werb Z, Bissell MJ. 1991. Proteinases of the mammary gland: developmental regulation in vivo and vectorial secretion in culture. Development 112:439–449.

Tan JL, Tien J, Pirone DM, Gray DS, Bhadriraju K, Chen CS. 2003. Cells lying on a bed of microneedles: an approach to isolate mechanical force. Proc Natl Acad Sci U S A 100:1484–1489.

Tominaga T, Ishizaki T, Narumiya S, Barber DL. 1998. p160ROCK mediates RhoA activation of Na-H exchange. EMBO J 17:4712–4722.

Van Essen DC, Drury HA, Joshi S, Miller MI. 1998. Functional and structural mapping of human cerebral cortex: solutions are in the surfaces. Proc Natl Acad Sci U S A 95:788–795.

Von den Hoff JW. 2003. Effects of mechanical tension on matrix degradation by human periodontal ligament cells cultured in collagen gels. J Periodontal Res 38:449–457.

Wei L, Roberts W, Wang L, Yamada M, Zhang S, Zhao Z, Rivkees SA, Schwartz RJ, Imanaka-Yoshida K. 2001. Rho kinases play an obligatory role in vertebrate embryonic organogenesis. Development 128:2953–2962.

Welsh CF, Roovers K, Villanueva J, Liu Y, Schwartz MA, Assoian RK. 2001. Timing of cyclin D1 expression within G1 phase is controlled by Rho. Nat Cell Biol 3:950–957.

Wicha MS, Liotta LA, Vonderhaar BK, Kidwell WR. 1980. Effects of inhibition of basement membrane collagen deposition on rat mammary gland development. Dev Biol 80:253–256.

Wirtz HR, Dobbs LG. 2000. The effects of mechanical forces on lung functions. Respir Physiol 119:1–17.

Wunnenberg-Stapleton K, Blitz IL, Hashimoto C, Cho KW. 1999. Involvement of the small GTPases XrhoA and XRnd1 in cell adhesion and head formation in early Xenopus development. Development 126:5339–5351.

Yamaguchi S, Yamaguchi M, Yatsuyanagi E, Yun SS, Nakajima N, Madri JA, Sumpio BE. 2002. Cyclic strain stimulates early growth response gene product 1-mediated expression of membrane type 1 matrix metalloproteinase in endothelium. Lab Invest 82:949–956.

Yan L, Moses MA, Huang S, Ingber DE. 2000. Adhesion-dependent control of matrix metalloproteinase-2 activation in human capillary endothelial cells. J Cell Sci 113:3979–3987.